Electron-Phonon Coupling Spectrum in Photodoped Pentacene Crystals

Mark Lee,* J. H. Schön, Ch. Kloc, and B. Batlogg
Bell Laboratories–Lucent Technologies, 600 Mountain Avenue, Murray Hill, New Jersey 07974

(Received 10 August 2000)

The coupling between conduction charges and the vibrational modes of the molecular lattice plays a defining role in the transport characteristics of organic semiconductors. Using electron tunneling spectroscopy, we obtain the electron–optical-phonon coupling spectrum in photodoped pentacene crystals at energies <30 meV. Comparison of the tunneling spectrum to infrared absorption data on the optical phonon density of states yields the energy dependence of the electron-phonon scattering matrix element. The integrated spectral weight of the electron-phonon coupling shows that superconductivity in pentacene is likely of electron-phonon origin.

DOI: 10.1103/PhysRevLett.86.862 PACS numbers: 72.80.Le, 63.20.Kr, 73.40.Gk

There is currently vigorous research activity in the use of organic semiconductor materials in thin film transistors [1]. Such "plastic" transistors can be made mechanically flexible and can be produced cheaply compared to standard transistors. At the same time, research into the properties of organic semiconductors has recently yielded fascinating new and unexpected scientific discoveries. Pentacene and tetracene, in particular, display a startling range of phenomena related to correlated electronic behavior. These are the only known materials that exhibit the quantum Hall effect [2] at low sheet densities (10^{11} to 10^{13} cm^{-2}), superconductivity [3] at high densities ($\sim 10^{14}$ cm^{-2}), and electrically pumped laser emission [4], all in the same high mobility crystals. Thus, there is clear need for a better understanding of the excitations and scattering processes in these semiconductors.

Organic semiconductors are structurally different from inorganic semiconductors such as Si. The polyacene family consists of strongly bonded aromatic molecules arranged on a lattice with weak van der Waals intermolecular bonds. The molecular lattice is easily polarizable, so it has been suggested for both oligothiophenes [5] and polyacenes [6] that the charge carriers are small polarons. Polarons are usually thought of as localized, though models for delocalized small polarons exist [7]. Studies [5] of dc conductivity in oligothiophenes showed a small mobility (<10 cm^2 V^{-1} s^{-1} from $4.2 < T < 300$ K) with a nonmonotonic T dependence. This was argued to be consistent with small polarons. However, the mechanism of polaron transport, i.e., inelastic hopping or band transport involving extended states, has been disputed. Very recent measurements [2,3] of Shubnikov–de Haas oscillations and of mobilities $\geq 10^4$ cm^2 V^{-1} s^{-1} (at 4.2 K) in very pure pentacene crystals prove that the charge carriers move as extended state wave functions in a metallic band. Clarifying the nature of possible polaron transport and superconductivity awaits more direct knowledge about the microscopic physics of the electron-phonon coupling in these materials.

Pentacene crystals were grown by sublimation in a continuous gas flow of 99.999 99% pure hydrogen. The horizontal flow growth apparatus and growth methods have been described in detail previously [8]. The gas flow allows very efficient purification of organic material. Additionally, crystals from the first growth were used as seed crystals for the second, crystals from the second used as seed for the third, etc. This results in iterative generational purification. In these crystals, the concentration of electrically active impurities was found [1] to be $\sim 10^{13}$ cm^{-3}.

Several pentacene crystals, roughly 5 mm by 1 mm by 0.1 mm thick, were glued onto sapphire substrates. Ohmic contacts were made to two ends of each crystal by evaporating 100 nm of Au. Each crystal was delaminated to expose a fresh surface prior to loading into another evaporator for Pb deposition. Tunnel junctions were fabricated by evaporating a series of Pb stripes (0.5 mm wide) across the top of each crystal perpendicular to its length, making sure that the Pb film was continuous over the sides (see Fig. 1, insets). The interface between Pb and pentacene formed a high-resistance barrier, the origin of which is not known. The pentacene was photodoped using two red ($\lambda_{\mathrm{peak}} = 635$ nm) light-emitting diodes, one mounted 2 mm above the sample and the other underneath the substrate. Our Hall effect measurements on photodoped pentacene show integer quantized Hall plateau, meaning that photodoping induces a quasi-two-dimensional sheet carrier density in the mid 10^{11} to 10^{12} cm^{-2}. Two-point resistances through the pentacene (with light) were 1 to 2 kΩ, while junction resistances were ~ 200 kΩ, showing that $>99\%$ of the voltage drop from pentacene to Pb occurred across the junction.

In a quantum tunneling experiment, bare electrons are injected into the pentacene from the Pb through a classically forbidden potential barrier. The electron is injected at energy eV, set by the voltage bias V, relative to the Fermi level (defined by $V = 0$). The tunneling current-voltage (I-V), conductance-voltage ($dI/dV - V$), and conductance derivative ($d^2I/dV^2 - V$) spectra are recorded. If the tunneling time is very fast compared to inverse scattering rates in the electrode, which is almost universally the case, then the dI/dV spectrum is proportional to the single-particle density of states for a bare charge at energy eV injected into the system. Note this is not necessarily the same as the density of states for a dressed quasiparticle, such as a polaron.

For superconducting electrodes like Pb, the electron-phonon coupling spectrum $\alpha^2(\omega)F(\omega)$, where $\alpha(\omega)$ is the magnitude of the electron-phonon scattering matrix integrated over momenta and $F(\omega)$ is the phonon density of states, produces characteristic structure in the energy gap function measured by tunneling. An integral equation inversion [9] is often used to deduce $\alpha^2(\omega)F(\omega)$ from d^2I/dV^2. For nonsuperconducting electrodes, electron-phonon coupling information can also be obtained by phonon-assisted tunneling [10]. In the simplest case, a tunneling electron injected at an energy resonant with a phonon mode in one electrode can scatter by simple phonon emission. d^2I/dV^2 is then proportional to a convolution of $\alpha^2(\omega)F(\omega)$ with a broadening function that both broadens and shifts the peak resonances [10]. Typically, the broadening and shifts are small, ~5% to 10%, so that $d^2I/dV^2 \propto \alpha^2(\omega)F(\omega)$ to good approximation. These phonon emission peaks in d^2I/dV^2 are usually antisymmetric with respect to bias polarity.

Definitive proof that the current between electrodes is due to quantum tunneling is given by observation of the Pb electrode's superconducting energy gap in dI/dV well below $T_c = 7.2$ K. This is shown for a Pb-pentacene junction in the inset of Fig. 1. The subgap conductance at $V = 0$ is consistent with thermal activation, showing that there are negligible nontunneling leakage current paths at low energies. The overall I-V does not have the strong bias asymmetry expected for a Schottky tunnel barrier, so the tunnel barrier may arise from a reaction between the Pb and the pentacene whose nature is unknown at this time.

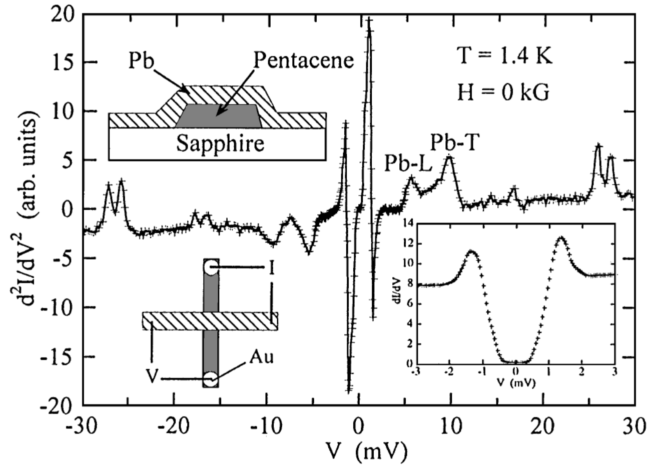

FIG. 1. Conductance derivative spectrum of a pentacene-Pb tunnel junction. Data were taken at $T = 1.4$ K in zero magnetic field. The large structure at $|V| < 3$ mV is due to the Pb superconducting energy gap. The Pb transverse (Pb-T) and longitudinal (Pb-L) phonon structures on the positive bias side are marked. Inset: (Left side) Schematic illustrations, not to scale, of the cross section (upper) and plan view (lower) of the Pb-pentacene junctions and the I-V wiring. (Lower right) Tunneling conductance spectrum of this junction showing the Pb superconducting density of states.

Figure 1 shows a d^2I/dV^2 spectrum for a pentacene-Pb junction at 1.4 K with the Pb superconducting. The large structure at $|V| < 3$ mV is from the Pb superconducting energy gap. The antisymmetric peaks near ±6 mV and ±10 mV marked Pb-T and Pb-L are the transverse and longitudinal phonon $\alpha^2(\omega)F(\omega)$ resonances of Pb. All energy scales are pushed out by the Pb energy gap of 1.3 mV. The resonant structures at higher energy are attributable to the pentacene. These features are symmetric with respect to bias polarity. Strong junction leakage sets in at biases above ~40 mV, probably due to deformation of the tunneling barrier, limiting the highest reliably measured tunneling energy to about 30 mV.

The pentacene structure in d^2I/dV^2 is shown more clearly in Fig. 2(a), where the Pb has been driven normal by a 2 kG magnetic field, eliminating any structure and gap offset due to the Pb superconductivity. The remaining peaks are from pentacene. These resonances can be compared to infrared absorption measurements, shown in Fig. 2(b). The optical spectrum clearly shows the IR-active phonon modes and provides a measurement

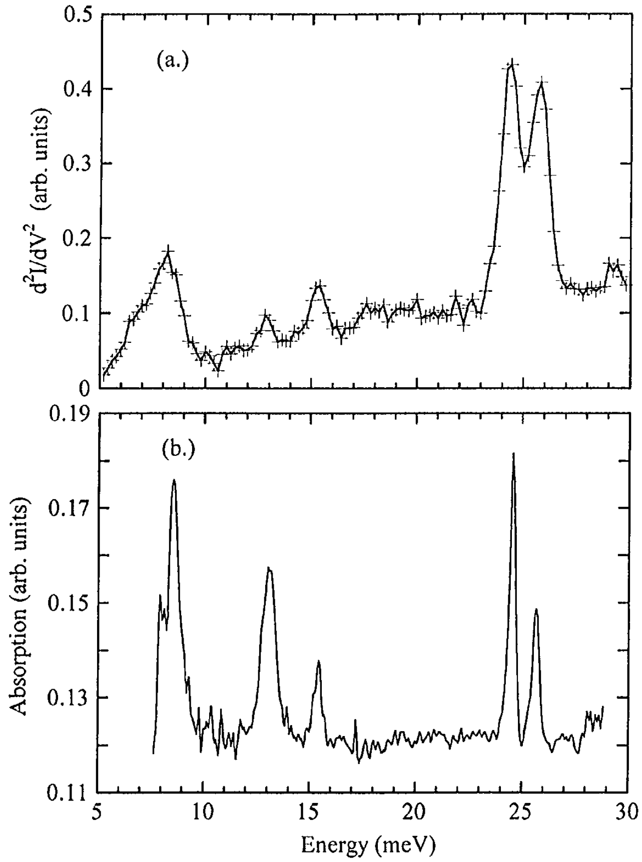

FIG. 2. (a) Conductance derivative spectrum of a pentacene-Pb tunnel junction at $T = 1.4$ K with the Pb driven nonsuperconducting by a 2 kG magnetic field. Under these conditions, all the resonant structure in the spectrum is due to the pentacene. (b) Infrared absorption spectrum of a pentacene crystal. The peaks are optical phonon modes with wave vector $q = 0$.

of $F_{q=0}(\omega)$, the optical phonon density of states at the Brillouin zone center. There is nearly a one-to-one correspondence in peak position between the tunneling and IR-active modes, proving that the tunneling peaks arise from electron-phonon coupling, and not from inelastic scattering by barrier impurities.

The symmetry of pentacene's electron-phonon peaks with respect to bias polarity in Fig. 1 means that the scattering is not simple phonon emission. In many degenerate semiconductors [11] peaks in d^2I/dV^2 symmetric with polarity have been observed near known optical phonon energies where the charge-phonon coupling is very strong. In most cases this is thought to arise from deformation potential coupling [12]. The symmetry of the scattering peaks arises from a modification of the charge dispersion and self-energy that is consistent with the conditions necessary for polaron formation [13], though it does not by itself prove the existence of polarons.

There are two obvious differences between the tunneling and optical spectra. First, the tunneling peaks have different relative intensities compared to the optical resonances. This arises mostly from the matrix element $\alpha^2(\omega)$, which weights the tunneling but not the optical spectrum. The relative energy dependence of $\alpha^2(\omega)$ can be separated from $F(\omega)$ by normalizing the tunneling spectrum to the optical spectrum, as shown in Fig. 3. Here values of the relative peak heights in the tunneling and optical data were separately normalized to the largest peak in each respective spectrum (after subtracting out a continuous background). Then the normalized tunneling spectrum peaks were normalized again against the corresponding optical spectrum resonances. Since the peak at 24 meV is the largest in both spectra, this procedure defined a value $\alpha^2(24 \text{ meV}) = 1$, and $\alpha^2(\omega)$ at other energies are measured relative to this. The second difference is that the tunneling peaks are broader than optical resonances. Thermal smearing and inelastic lifetime contribute some to the tunneling peak widths. Also, unlike photons, electrons can couple to phonon modes away from the zone center. Hence any dispersion of the phonon modes will appear as an additional energy width in the electronic spectrum.

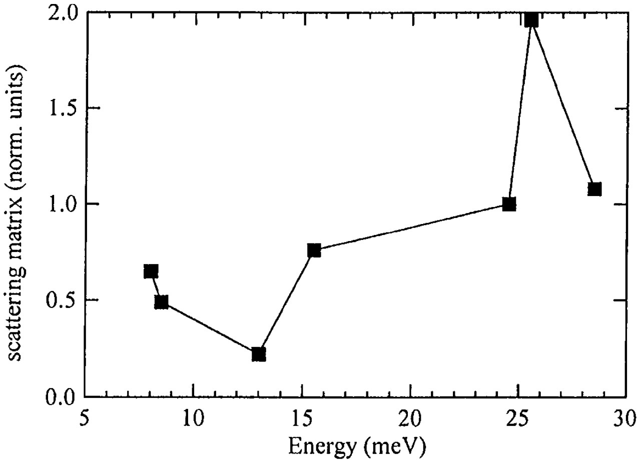

FIG. 3. Relative energy dependence of the squared magnitude of the electron-phonon scattering matrix element $\alpha^2(\omega)$. The values are normalized so that $\alpha^2(\omega = 24 \text{ meV})$ is defined as unity.

Although no phonon mode assignments have been made to date specifically for pentacene, the similarity in its infrared absorption spectrum to other molecular crystals suggests [14] that all structure below 20 meV arise from intermolecular vibrations. These are the ordinary phonon modes common to all crystalline solids. The origin of the strong double peaks around 25 meV is less clear. It is possible these peaks may be the lowest energy intramolecular vibrations of the ring molecules, or may be some hybridization of inter- and intramolecular motion.

The presence of the strong electron-phonon peaks in Figs. 1 and 2 proves that electron-phonon scattering plays a fundamentally important role in pentacene's transport. To understand the superconductivity better, it is useful to estimate the dimensionless electron-phonon coupling constant λ, which is defined as

$$\lambda = \int \alpha^2(\omega)F(\omega)\omega^{-1}\,d\omega\,. \tag{1}$$

While numerical integration of the pentacene resonances in d^2I/dV^2 (after a background correction) is straightforward, the units of d^2I/dV^2 are not physically meaningful, so getting an absolute value of $\lambda_{\text{pentacene}}$ requires a normalization [15]. For simplicity, we approximate $\lambda_{\text{pentacene}}/\lambda_{\text{Pb}}$ by normalizing the integral of the pentacene resonances to the integral of the Pb phonon structure in the same spectrum, averaged over both bias polarities. This assumes that the integral of the Pb-T and Pb-L peaks in $d^2I/dV^2 \propto \lambda_{\text{Pb}}$. In fact, in a superconductor d^2I/dV^2 is formally proportional to a complicated integral function of $\alpha^2(\omega)F(\omega)$ convoluted with the superconducting gap function. Above the sharp gap peak structure (~3 mV here), the gap function is relatively slowly varying. Our simplification then amounts to linearizing the relation between d^2I/dV^2 and $\alpha^2(\omega)F(\omega)$ in Pb, at least over the small energy range where the Pb phonon structure is prominent. Using this approximation, we can use the known value [16] $\lambda_{\text{Pb}} = 1.55$ to estimate $\lambda_{\text{pentacene}} \sim 0.7\lambda_{\text{Pb}} = 1.1$. We emphasize that this value is an estimate, but it is very close to a value $\lambda_{\text{pentacene}} = 1.2$ obtained independently as a fitting parameter from a fit [17] of the mobility's temperature dependence to deformation potential scattering [13], using an analysis reported previously [18].

The electron-phonon data can be inserted into the formula for the transition temperature T_c derived from the Eliashberg formalism for superconductivity [19]:

$$T_c = \langle \hbar\omega_{\log}\rangle \exp\left(-\frac{1.04(1 + \lambda)}{\lambda - \mu^*(1 + 0.62\lambda)}\right), \tag{2}$$

where $\langle \hbar\omega_{\log}\rangle$ is a logarithmically weighted average of the phonon mode energies and μ^* is a parameter describing the strength of the retarded Coulomb repulsion. From the data for pentacene, we find $\langle \hbar\omega_{\log} \rangle = 190 \pm 10$ K. Using $\lambda = 1.1$, the only parameter not obtainable from data is μ^*. Theoretical analyses [20] argue that all the aromatic molecular crystals should have μ^* in the range 0.3 to 0.4. Inserting these values into Eq. (2) yields a calculated range of $1 < T_c < 5$ K. This compares very well with the measured [3] T_cs of 1.8 K for pentacene and 2.4 K for tetracene, providing very strong evidence that the superconductivity is electron-phonon based.

The above analysis does not account for two possible complications. First, the quantum Hall effect and an anisotropy of $>10^2$ between in-plane and out-of-plane mobility mean that the charge carriers form a quasi-two-dimensional system, whereas Eq. (2) is from a 3D formalism. Second, the tunneling spectrum is at a much lower density ($\sim 10^{12}$ cm^{-2}) than that for which superconductivity is observed ($\sim 10^{14}$ cm^{-2}), so it is not obvious that our λ can be extended to the superconducting state. These issues can be related. The 2D nature makes the density of states independent of carrier density. Hence λ, which depends implicitly on the density of states, becomes density independent, so that the tunneling value is applicable to the superconductivity analysis. We assume that λ depends on density only through the density of states. This argument is invalid if some other aspect of the electron-phonon physics differs significantly at high density, but there is as yet no evidence for such a phenomenon.

Finally, the dimensionality issue affects the interpretation of μ^*. The value of μ^* used in the analysis of T_c is over twice what is found in all superconducting metals. Some opposing theoretical assessments [21] argue for a more conventional value of $\mu^* \sim 0.15$ in aromatic molecular crystals. Using Eq. (2) such a value of μ^* would increase the calculated T_c to 12 K. However, thermodynamic fluctuations of the superconducting order parameter (not included in the Eliashberg theory) will eventually drive T_c down to zero as the dimensionality is reduced from bulk 3D to the strict 2D limit [22]. Thus it is possible that pentacene may have a more standard value of μ^* but a lower T_c than derived from Eq. (2) due to its lower effective dimensionality. Nonetheless, questions about μ^* do not change our basic conclusion that the superconductor pairing mechanism is based on electron-phonon coupling.

In summary, electron tunneling spectroscopy has been used to measure the electron-phonon coupling spectrum in photodoped pentacene crystals. Resonances in the tunneling spectrum occur at the same energies as known optical phonon modes. The symmetry of the resonances indicates that the electron-phonon scattering strongly modifies the dispersion and self-energy functions. An estimate for the electron-phonon coupling parameter from the data gives $\lambda \sim 1.1$. Using this λ and the known phonon energies, the mechanism of superconducting pairing in pentacene can be determined to be electron phonon.

We thank C. M. Varma and P. B. Littlewood for useful discussions and S. Berg for help generating the infrared absorption spectrum.

---

*Electronic mail: markl@lucent.com

[1] G. Horowitz, Adv. Mater. **10**, 365 (1998); H. E. Katz, Z. Bao, and A. Dodabalapur, *Handbook of Oligo- and Polythiophenes,* edited by D. Fichou (Wiley-VCH, Weinhelm, Germany, 1998), pp. 459–489; J. H. Schön, S. Berg, C. Kloc, and B. Batlogg, Science **287**, 1022 (2000).

[2] J. H. Schön, C. Kloc, and B. Batlogg, Science **288**, 2338 (2000).

[3] J. H. Schön, C. Kloc, and B. Batlogg, Nature (London) **406**, 702 (2000).

[4] J. H. Schön, Ch. Kloc, A. Dodabalapur, and B. Batlogg, Science **289**, 599 (2000).

[5] L. Torsi, A. Dodabalapur, L. J. Rothberg, A. W. P. Fung, and H. E. Katz, Science **272**, 1462 (1996); M. W. Wu and E. M. Conwell, Chem. Phys. Lett. **266**, 363 (1997).

[6] E. A. Silinsh and V. Capek, *Organic Molecular Crystals* (AIP Press, New York, 1994).

[7] T. Holstein, Ann. Phys. **8**, 343 (1959).

[8] Ch. Kloc, P. G. Simpkins, T. Siegrist, and R. A. Laudise, J. Cryst. Growth **182**, 416 (1997); R. A. Laudise, Ch. Kloc, P. G. Simpkins, and T. Siegrist, J. Cryst. Growth **187**, 449 (1998).

[9] E. L. Wolf, *Principles of Electron Tunneling Spectroscopy* (Oxford University Press, New York, 1985), pp. 236–280.

[10] Wolf, *Principles of Electron Tunneling Spectroscopy* (Ref. [9]), pp. 339–348.

[11] E. L. Wolf, Phys. Rev. Lett. **20**, 204 (1968); D. C. Tsui, Phys. Rev. Lett. **21**, 994 (1968); F. Steinresser, L. C. Davis, and C. B. Duke, Phys. Rev. **176**, 912 (1968).

[12] L. C. Davis and C. B. Duke, Solid State Commun. **6**, 193 (1968).

[13] J. Appel, in *Solid State Physics,* edited by F. Seitz, D. Turnbull, and H. Ehrenreich (Academic Press, New York, 1968), Vol. 21.

[14] G. Cerullo, G. Lanzani, M. Muccini, C. Taliani, and S. De Silvestri, Phys. Rev. Lett. **83**, 231 (1999); T. A. Krivenko, V. A. Dmentjev, E. L. Bokhenkov, A. I. Kolesnikov, and E. F. Sheka, Mol. Cryst. Liq. Cryst. **104**, 207 (1984).

[15] Since the pentacene in our junctions is not superconducting, we cannot obtain a dimensionless scale by normalizing d^2I/dV^2 against its BCS superconductor gap structure, as is done for a conventional superconductor.

[16] R. C. Dynes and J. M. Rowell, Phys. Rev. B **11**, 1884 (1975).

[17] J. H. Schön (unpublished).

[18] J. H. Schön, C. Kloc, and B. Batlogg, Synth. Met. **115**, 75 (2000).

[19] P. B. Allen and R. C. Dynes, Phys. Rev. B **12**, 905 (1975).

[20] A. Devos and M. Lannoo, Phys. Rev. B **58**, 8236 (1998); O. Gunnarsson, Rev. Mod. Phys. **69**, 575 (1997).

[21] C. M. Varma, J. Zaanen, and K. Raghavachari, Science **254**, 989 (1991).

[22] M. R. Beasley, J. E. Mooij, and T. P. Orlando, Phys. Rev. Lett. **42**, 1165 (1979); B. I. Halperin and D. R. Nelson, J. Low Temp. Phys. **36**, 599 (1979).